Biogeosciences Discussions

Whole water column distribution and carbon isotopic composition of bulk particulate organic carbon, cholesterol and brassicasterol from the Cape Basin to the northern Weddell Gyre in the Southern Ocean

A.-J. Cavagna[1], F. Dehairs[1], V. Woule-Ebongué[1], S. Bouillon[2], F. Planchon[3,*],
B. Delille[4], and I. Bouloubassi[5]

[1]Earth and System Sciences & Analytical and Environmental Chemistry, Vrije Universiteit
Brussel, Brussels, Belgium
[2]Department of Earth and Environmental Sciences, Division of soil and water management,
Katholieke Universiteit Leuven, Leuven, Belgium
[3]Department of Geology and Mineralogy, Section of Mineralogy and Petrography,
Royal Museum of Central Africa, Tervuren, Belgium

Title Page

Abstract	Introduction
Conclusions	References
Tables	Figures

◄◄	►►
◄	►
Back	Close

Full Screen / Esc

Printer-friendly Version

Interactive Discussion

[4]Départment d'Astrophysique, Geophysique et Océanographie/Océanographie chimique, Université Libre de Liège, Liège, Belgium
[5]Laboratoire d'Océanographie et du Climat (LOCEAN), Université Pierre et Marie Curie, Paris, France
[*]now at: Laboratoire des Sciences de l'Environnement Marin (LEMAR), Institut Universitaire Européen de la Mer, Plouzané, France

Correspondence to: A.-J. Cavagna (acavagna@vub.ac.be)

Title Page

Abstract | Introduction

Conclusions | References

Tables | Figures

◄ | ►

◄ | ►

Back | Close

Full Screen / Esc

Printer-friendly Version

Interactive Discussion

Abstract

The combination of concentrations and δ^{13}C signatures of Particulate Organic Carbon (POC) and sterols provides a powerful approach to study ecological and environmental changes both in the modern and ancient ocean, but its application has

5 so far been restricted to the surface area. We applied this tool to study the biogeochemical changes in the modern ocean water column during the BONUS-GoodHope survey (Feb–Mar 2008) from Cape Basin to the northern part of the Weddell Gyre. Cholesterol and brassicasterol were chosen as ideal biomarkers of the heterotrophic and autotrophic carbon pools, respectively, because of their ubiquitous and relatively

10 refractory nature.

We document depth distributions of concentrations (relative to bulk POC) and δ^{13}C signatures of cholesterol and brassicasterol from the Cape Basin to the northern Weddell Gyre combined with CO_2 aq. surface concentration variation. While relationships between surface water CO_2 aq. and δ^{13}C of bulk POC and biomarkers have been pre-

15 viously established for surface waters, our data show that these remain valid in deeper waters, suggesting that δ^{13}C signatures of certain biomarkers could be developed as proxies for surface water CO_2 aq. Our data suggest a key role of zooplankton fecal aggregates in carbon export for this part of the Southern Ocean. We observed a general increase in sterol δ^{13}C signatures with depth, which is likely related to a combination

20 of particle size effects, selective feeding on larger cells by zooplankton, and growth rate related effects Additionally, in the southern part of the transect south of the Polar Front (PF), the release of sea-ice algae is hypothesized to influence the isotopic signature of sterols in the open ocean. Overall, combined use of δ^{13}C and concentrations measurements of both bulk organic C and specific sterol markers throughout the water

25 column shows the promising potential of analyzing δ^{13}C signatures of individual marine sterols to explore the recent history of plankton and the fate of organic matter in the SO.

1 Introduction

The intensity of organic matter export combined with the efficiency of deep water heterotrophic reprocessing of this material sets the sequestration's efficiency of the oceanic biological carbon pump (Honjo et al., 2008; Boyd and Trull, 2007; Battle et al., 2000). However, it appears difficult to balance the organic C demand by twilight zone heterotrophs (currently defined as 100–1000 m) by the export flux from the upper mixed layer (Burd et al., 2010; Steinberg et al., 2008; Reinthaler et al., 2006; Arístegui et al., 2005). Therefore it is essential to better understand the processes controlling the export and reprocessing of exported OM (Boyd and Trull, 2007). Gaining information about the sources and fate of sinking and suspended biogenic particles is necessary to improve our knowledge on what is happening below the euphotic layer, where the attenuation of the export flux is the strongest. Wakeham et al. (2009) state that one way to improve our understanding about mechanisms controlling interrelated biogeochemical processes involved in particle sinking and decomposition is to determine the chemical compositions of those particles sinking rapidly through the water column as well as of the suspended fine particles with longer residence time.

While several studies have examined the δ^{13}C of the bulk particulate organic carbon (POC) in the Southern Ocean (Lourey et al., 2004; Trull and Armand, 2001; Popp et al., 1999; Bentaleb et al., 1998; Dehairs et al., 1997; Rau et al., 1997; Kennedy and Robertson, 1995; François et al., 1993), fewer studies have focused on specific compounds. O'Leary et al. (2001); Tolosa et al. (1999) and Popp et al. (1999) report on the factors controlling the carbon isotopic composition of phytoplankton based on the study of δ^{13}C$_{POC}$, δ^{13}C$_{sterols}$ and δ^{13}C$_{phytol}$. Both these studies, however, were mainly limited to an investigation of the surface particles, so the distribution of these biomarkers in deeper waters remains unknown. To the best of our knowledge, no information is available on specific compounds and their isotopic composition for the intermediate and deep Southern Ocean. However, identifying the food web components controlling the C flux in the deeper water column and understanding compositional changes

of suspended and sinking organic material is important to better constrain the fate of organic matter exported to the deep ocean. We investigated this by studying the variability in concentration of individual compounds and their ^{13}C isotopic composition.

While cholesterol ($27\Delta^5$; cholest-5-en-3β-ol) is produced by some algae (Volkman, 2003; 1986) it is commonly considered as a biomarker for consumer organisms and a proxy for zooplanktonic herbivory (Grice et al., 1998). Schouten et al. (1998) propose cholesterol as a general biomarker for the eukaryotic marine community, thereby avoiding the complexity inherent to species-specific sterols that have different isotopic offsets relative to phytoplankton δ^{13}C. A general biomarker averages out the effects due to variability of biosynthetic pathways, cell size, geometry, and growth rate between individual species. Grice et al. (1998) show via controlled mesocosm experiments that grazers convert different algal precursor sterols into cholesterol without significant isotopic fractionation. Moreover, Chikarahishi (2006) in accordance with Grice et al. (1998) suggest that no substantial carbon isotopic fractionation occurs during either heterotrophic sterol assimilation or de novo synthesis.

Schouten et al. (1998) state that the refractory nature and ubiquitous character of cholesterol as an eukaryotic marker should favor the integrity of the δ^{13}C$_{cholesterol}$ signatures when particles sink to greater depth, thereby preserving the information acquired in surface waters. Brassicasterol ($28\Delta^{5,22}$: 24-Methylcholesta-5,22E-dien-3β-ol) is reported in a large number of algal classes (Volkman, 2003; 1986) and is considered as a strict phytosterol, i.e. it cannot be biosynthesized by zooplankton. For these reasons, it is commonly used as an indicator of marine algae and of diatoms in particular in the environment. Recently, Rampen et al. (2010) stressed that when diatoms dominate the phytoplankton community, sterols, and brassicasterol in particular (abundant in the pennate diatoms) provide useful information on the type of diatoms that are present. Therefore, for the Southern Ocean where diatoms are dominant but where other phytoplankton groups contribute to the primary production, we will consider brassicasterol as a strict phytoplankton indicator. Because of their ubiquitous and relative refractory nature (e.g. Volkman, 1986, 2003), cholesterol and brassicasterol were thus

chosen in this study as ideal markers of the heterotrophic and autotrophic carbon pools that have potential for being sequestered in the deep ocean.

As a part of a broader study on the biogeochemistry and C fluxes along the Greenwich Meridian, we document variations in concentration (relative to bulk POC) and δ^{13}C compositions of cholesterol and brassicasterol over the whole water column from the Cape Basin to the northern Weddell Gyre. Combined with data on $CO_{2aq.}$ concentrations, our results furthermore enable to verify earlier surface waters observations about CO_2 substrate concentration and C isotopic composition of bulk POC and biomarkers. They also document to what extent this substrate-dependent C isotopic signature, acquired in the surface is preserved deeper in the water column. This is important since particles may, or may not, become isotopically homogenous at depth as a result of mixing, depending on magnitude of sinking velocity relative to advection. This comes to answering the question whether the system is operating in 1-D (strong surface to deep links) or 3-D (strong mixing and homogenization in the deep ocean) configuration.

2 Materials and methods

2.1 Sampling and hydrology

The "Biogeochemistry in the Southern Ocean: Interactions between Nutrients, Dynamics and Ecosystems Structures" (BGH) expedition took place in the South East Atlantic and the Atlantic sector of the Southern Ocean during summer 2008 (February-March 2008) on board R/V *Marion Dufresne* (voyage track showed in Fig. 1). The BGH project in the region south of South Africa was built on two main objectives related to: (1) the large scale inter-ocean exchanges and (2) the characterization of the biogeochemical processes involved in the internal cycling of trace elements, isotopes and carbon. South of Africa, the Southern Ocean (SO) provides the export channel for North Atlantic Deep Water (NADW) to the global ocean and the passage for heat and

salt water from the Indian and Pacific oceans. The eastward flowing Antarctic Circumpolar Current (ACC), the South Atlantic Current and NADW meet with the westward flow of Indian waters carried by the Agulhas Current, leading to water mass exchanges through jets, meanders, vortices, and filament interactions. Indeed, the Agulhas Cur-

5   rent is the major western boundary current of the Southern Hemisphere (Lutjeharms, 2006) and a key component of the global ocean "conveyor" circulation controlling the return flow to the Atlantic Ocean (Gordon, 2003; 1986). Unusual dynamics pervade the motion of this warm-water current – as it moves west around the Southern tip of Africa, it is reflected back east by the ACC. Not all waters are captured by this sudden diver-

10   sion of course – parts of the Agulhas Current leak away into the South Atlantic Ocean (BGH cruise report). However, the ACC fronts (Fig. 1) represent almost impermeable barriers delimiting zones with relatively constant hydrological and biogeochemical properties, and lower baroclinic transport (Sokolov and Rintoul, 2007). Cross frontal exchanges occur but mainly locally close to sharp topographic features. Water par-

15   ticles spend several years in each zone before to be advected northward by Ekman pumping, and subsequently take part in several winter convective mixings (S. Speich, personal communication, 2009).

Amongst the sites studied during BGH, five sites had sufficient station occupation time (about 48 h) to enable whole water column suspended matter sampling with High

20   Volume In Situ Filtration Systems (HVFS) because this operation is time consuming (6 to 8 h per deployment). Up to a maximum of 12 HVFS units were deployed covering the entire water column from the surface to the deep ocean. The five sites were selected to cover the major zonal systems framed by fronts (Fig. 1). The complete salinity and temperature sections during BGH are available in Fig. 1.

25   Suspended particulate organic matter was sampled using in situ large volume filtration systems (Challenger Oceanics and McLane WTS6-1-142LV systems) fitted with 142 mm diameter filters holders. Water was pumped through two successive filters: (i) a 53 µm mesh nylon screen (filter SEFAR-PETEX®; polyester) and (ii) a QM-A quartz fiber filter (∼1 µm porosity, Pall Life). Prior to use PETEX screens were conditioned by

soaking in HCl 5 %, rinsed with Milli-Q grade water, dried at ambient temperature under a laminar flow hood and were stored in clean plastic zip-bags till use. QMA filters were conditioned by combustion at 450 °C during 4h and were stored in clean plastic zip-bags till use.

5　Since the suspended matter samples were also intended for analysis of ^{234}Th (Planchon et al., this issue), filters were partitioned among the different end-users, using sterile scalpels and a custom-build INOX steel support for the PETEX screens and a plexiglass punch of Ø = 25.3 mm for the QMA filters. These operations were conducted under a laminar flow hood. Whenever possible, both size fractions (>53 μm and 10　53≫1 μm) were sampled for biomarkers analyses. This was in general the case for the upper ocean mixed layer. Below the mixed layer, the large particle fraction (>53 μm) could not be recovered because screens carried too little material. Aliquots dedicated to compound specific isotope analysis (CSIA) were packed in cryotubes and stored at –80 °C till processing in the home-laboratory. Aliquots dedicated to the analysis 15　of δ^{13}C$_{POC}$ were dried at 50 °C and stored in Petri dishes at ambient temperature till processing in the home laboratory.

2.2　δ^{13}C$_{POC}$: sample preparation and analysis

POC concentrations and δ^{13}C$_{POC}$ were analyzed via elemental analyzer – isotope ratio mass spectrometer (EA-IRMS). Prior to this, inorganic carbon (carbonates) was 20　removed by exposing the filters to concentrated HCl vapor inside a closed-glass container during 4 h (Lorrain et al., 2003). After drying at 50 °C the samples were packed in silver cups and analyzed with a Thermo Flash 112 elemental analyzer configured for C analysis and coupled on-line via a Con-Flo III interface to a Thermo-Finnigan Delta V IRMS. Acetanilide and IAEA-CH-6 reference materials were used for calibrat-25　ing concentrations and isotopic composition, respectively. The bulk POC dataset for large (>53 μm Ø) and small (53≫1 μm Ø) particles is presented in Table 1.

2.3 $\delta^{13}C_{sterols}$: sample preparation and analysis

Samples were processed following the method described in Boschker (2004). Briefly, total lipids were extracted using a modified method from Bligh and Dyer (1959) with chloroform / methanol / Milli-Q water (v:v, 15:15:6 mL) mixture. Usually, 70 to 80 % of the chloroform phase containing the total lipid fraction was recovered, implying that true concentrations are 20 to 30 % underestimated (*Boschker, 2004*).

Since the final standard error on the $\delta^{13}C$ measurements is estimated to range between 1.1 and max 2.0‰, and because this extraction step implies permanent sample shaking to homogenize and optimize recovery of the extract, we assume that isotopic bias due to incomplete recovery is negligible compared to the actual accuracy and precision of the measurement.

The total lipid extract was then separated into neutral, glyco-, and polar lipids on silica chromatographic column (0.5 g Kieselgel 60; Merck): (i) the neutral phase was eluted with chloroform (7 mL), (ii) the glycolipidic phase with acetone (7 mL), and (iii) the polar phase with methanol (10 mL). The glycolipidic and the polar phases were stored at −20 °C while the neutral phase was immediately processed for analysis.

Neutral phases were completely dried under gentle inert N_2 flow (to avoid degradation) while the glyco-lipids and the polar phases were stored at −20 °C for further analyses; and a known quantity of squalane used as internal standard (IS, i.e., a stable compound which does not co-elute with natural compounds present in the samples) was added. To estimate compound concentrations in the samples, we use as reference the GC-c-IRMS peak area of squalane since the added IS amount is known.

To increase volatility and enhance thermal stability of sterols for their separation by gas chromatography (e.g. Lagarda et al., 2006), dried neutral lipids were derivatized using bis-(trimethylsilyl)-trifluoroacetamide (BSTFA, 99 %)/toluene (v:v, 1:1). Trimethylsylil (TMS) groups are substituted to the hydrogen of the hydroxyl groups of the compounds to form trimethylsyliloxy groups [-O-Si-$(CH_3)_3$]. In practice, derivatization is achieved by adding 50 µL of BSTFA-toluene to the dried samples (and squalane) and heating during 60 min at 60 °C.

Title Page

Abstract | Introduction

Conclusions | References

Tables | Figures

◄ | ►

◄ | ►

Back | Close

Full Screen / Esc

Printer-friendly Version

Interactive Discussion

All the TMS-derivatized neutral fractions (+ IS) were analyzed using a Trace GC Ultra coupled to Trace Plus MS (Interscience) for compound identification and a Thermo Finnigan GC equipped with a combustion furnace (CuO/NiO/Pt reactor at 940 °C) coupled to a Delta*Plus* XL isotope ratio mass spectrometer (IRMS), for δ^{13}C and con-
⁵ centration measurements. Compound identification was achieved by (i) retention time matching between standard mix and sample, (ii) GC-MS mass spectrometry characterization (matching with Goad and Akihisa, 1997).

Both gas chromatographs were equipped with similar capillary columns [DB-5-type (J&W Scientific), 30 m × 0.32 mm i.d. with 0.25 μm film thickness]. Identical tempera-
¹⁰ ture programming was used for both GC ovens starting from 50 °C (2 min) to 300 °C (15 min) with a ramp of 4 °C min^{-1}. Carrier gas flow (He) was 2 mL min^{-1}, and injection occurred in splitless mode at 300 °C. Blanks (hexane) and mixtures of standards were regularly measured in between sample analyses (standard bracketing) to check the stability of the systems and absence of possible contaminants.

¹⁵ The carbon isotopic composition of squalane (internal standard), treated similarly as the samples (extracted neutral phase), was used to check reproducibility and accuracy of the GC-c-IRMS system. Aliquots of 0.5 mg squalane powder are weighed into tin capsules (IVA, 3.3 × 5 mm) and analyzed via EA-IRMS (Thermo) using IAEA-CH$_6$ as reference material. A good agreement is observed between the mean $\delta^{13}C_{squalane}$
²⁰ obtained via EA-IRMS ($\delta^{13}C_{squalane}$ = −20.2 ± 0.1 ‰, 1σ, n = 3) and GC-c-IRMS ($\delta^{13}C_{squalane}$ = −21.2 ± 0.9 ‰, 1σ, n = 69).

Due to the addition of a trimethylsylil group to each individual compound (TMS-derivatization), the δ^{13}C of cholesterol (27Δ^5; cholest-5-en-3β-ol) and brassicast-erol (28Δ^{5,22}; 24-Methylcholesta-5,22E-dien-3β-ol) obtained from GC-c-IRMS need to
²⁵ be corrected. Five standards: 5α-cholestane, cholesterin-α24, stigmasterol-α22, β-sitosterol, 7-dehydrocholesterol are used for this purpose. Comparison between mean δ^{13}C measured by GC-c-IRMS on derivatized (n = 3) and non-derivatized (n = 3) standards' mix is achieved using a functional relationship estimation by maximum likelihood

(FREML) (Fig. 2a) via Eq. 1:

$$\delta^{13}C_{\text{sterol}} = \frac{(n+3) \times \delta^{13}C_{TMS-sterol} - 1 \times \delta^{13}C_{BSTFA}}{n} \tag{1}$$

Where $\delta^{13}C_{\text{sterol}}$ is the measured carbon isotopic signature of non-derivatized standard sterol, n is the number of replicates, $\delta^{13}C_{TMS-sterol}$ is the measured carbon isotopic signature of derivatized standard sterol and $\delta^{13}C_{BSTFA}$ is the measured carbon isotopic signature of BSTFA-toluene used to derivatize sterols.

Since no certified reference materials for compound-specific stable isotope measurements exist, we furthermore compare mean $\delta^{13}C$ measured by GC-c-IRMS and EA-IRMS of the same non TMS-derivatized compounds ($n = 3$) (Fig. 2B) and include it in the $\delta^{13}C_{\text{sterol}}$ correction following a FREML equation as described above (equation 1 applied for non-derivatized standard sterols analyzed either via EA-IRMS or via GC-c-IRMS).

Final $\delta^{13}C$ values for each compound are thereby corrected for isotopic deviation from TMS-derivatization, as well as possible isotopic deviation from GC-c-IRMS compared to EA-IRMS. The uncertainty on final $\delta^{13}C$ of cholesterol (cho) and brassicasterol (bra) ($\pm 1\sigma$; Tables 2 and 3) is calculated by propagating standard deviations from triplicate measurements (i.e. 1σ) and correction from derivatization.

3   Results

3.1   Contents of cholesterol, brassicasterol and POC-bulk

Results for POC (large and small particles), brassicasterol and cholesterol concentrations in the small (1≪53 μm) and large (>53 μm) particle size fractions and are listed in Tables 1, 2 and 3, respectively. Brassicasterol and cholesterol contents are of similar magnitude. Cholesterol was usually slightly less abundant than brassicasterol, but was detectable over the entire water column, while brassicasterol was undetectable

Full Screen / Esc

Printer-friendly Version

Interactive Discussion

(i.e. concentrations are below the GC-c-IRMS/GC-MS detection limit) in deeper water at the most northward stations S1 and S2.

Depth profiles of large particle POC (LP-POC) are shown relative to total POC (T-POC = LP-POC + SP-POC, where SP-POC is small particle POC) to highlight specific features of the profiles (Fig. 3, upper panel). To that purpose we also plotted the parameters vs. density rather than vs. depth. Depth profiles of small particles cholesterol (SP-cholesterol) and brassicasterol (SP-brassicasterol) are shown relative to SP-POC (Fig. 3, lower panel) following the same rationale.

3.1.1 General features

Relative contents of LP-POC and SP-sterols changed considerably in surface waters along the studied transect. Overall, the contributions of LP-POC ranged from 0.8 to 27.0 % of total POC, with highest values at S3 (27.0 %) in the Polar Frontal Zone (PFZ), and S5 (25.8 %) in the northern Weddell Gyre. LP-POC values often displayed a maximum in mesopelagic to deep waters. This maximum was clearly visible at S1 (750 m), S3 (450 m) but less prominent at S2 (250 m) and absent at S4 (Fig. 3, upper panel). At S5, an LP-POC maximum was present at 1500 m, below the mesopelagic layer. With the exception of station S4, a systematic increase of LP-POC over T-POC ratio was apparent near the seafloor (nepheloid layer), ranging between 2.7 % (station S1) and 12.3 % (station S2). The large error bars (up to 100 %) in Fig. 3 reflected the large variability between close-by sampled depths (see also Tables 1, 2) reflecting both heterogeneity of the system (as an example, close-by depths were often sampled with an interval of 24 h) and variability due to analytical method.

Profiles of relative SP-cholesterol and SP-brassicasterol contents (Fig. 3, lower panel) were also characterized by mesopelagic maxima, except at S1 where brassicasterol below 750 m was under detection limit and at S4 where no mesopelagic maximum was present. The depths of mesopelagic maxima for cholesterol and brassicasterol were rather similar between sites, and ranged between circa 200 and 800 m (Fig. 3 lower panel). The highest brassicasterol contents were observed at S1 and S5

in good accordance with the presence of the diatom pigment fucoxanthin in surface water (J. Ras, personal communication, 2009). Below the mesopelagic maximum the relative contents of cholesterol and brassicasterol decreased toward the seafloor (S1, S2, S3; Fig. 3 lower panel), or remained rather unchanged (S4, S5). In contrast to rel-
5 ative contents of LP-POC, no increase of brassicasterol and cholesterol contents was observed near the seafloor.

3.1.2 Site specific features

The surface waters at station S1 showed the highest (relative) SP-brassicasterol content and also the highest concentration ($65.3\,\mathrm{ng\,L^{-1}}$) of the whole dataset (Fig. 3
10 and Table 2). This is in accordance with the observed high concentrations of Chl-a and phaeopigments (Le Moigne et al., 2012). The profiles of relative SP-cholesterol and LP-POC contents at S1 were quite similar, with pronounced surface and broad mesopelagic maxima: the latter reached circa 100 % of the surface content for cholesterol, and circa 40 % for LP-POC.
15   Station S2, which was also located in the area of high Chl-a and phaeopigment concentrations, north of the Sub-Antarctic Front (SAF) (Le Moigne et al., this issue), showed LP-POC contents relatively similar than at S1. Here surface water brassicasterol reached its second highest value ($46.8\,\mathrm{ng\,L^{-1}}$; Table 2) for the entire cruise, in agreement with the high chloropigments concentrations (J. Ras, personal communica-
20 tion, 2009). The mesopelagic maximum of relative cholesterol and brassicasterol contents, located at about 600 m, was pronounced and sharp, whereas relative content of LP-POC shows a weak mesopelagic maximum expanding from 200 to 1000 m (Fig. 3). At this site the increase of LP-POC in approach of the seafloor was the strongest (reaching up to 12 % of total POC) of the entire survey.
25   At S3 the mesopelagic LP-POC content was the highest of the entire section (Fig. 3). A clear broad mesopelagic maximum of LP-POC and SP-cholesterol content was present between 500 and 600 m. SP-brassicasterol showed a weak maximum

Selected sterols and their δ^{13}C in the Southern Ocean water column

A.-J. Cavagna et al.

expanding from the near-surface water to 600 m. Again, profiles of LP-POC and SP-cholesterol relative contents were quite similar.

Station S4 was located above the Atlantic-Indian ridge in an area with lowest Chl-*a* and phaeopigment concentrations (Le Moigne et al., this issue). At this site, no mesopelagic maximum was observed and depth profiles of SP-sterols and LP-POC were quite similar. The maximum relative content of SP-sterols and LP-POC was meanwhile located closer to the surface, at 80 m.

Station S5 was characterized by deep reaching Chl-*a* concentrations (circa 150 m) and small sub-surface (100–125 m) phaeopigment concentration (Le Moigne et al., this issue). Surface waters showed the highest relative content of LP- POC (Fig. 3) and also the highest total POC concentrations (up to 25.8 µg l^{-1}; Table 1) of the entire cruise. A second LP-POC maximum was present at 1500 m (Fig. 3). The relative contents of brassicasterol and cholesterol showed a sharp mesopelagic maximum ranging between 300 to 500 m. Brassicasterol showed a second smaller maximum at 1500 m, coinciding with the LP-POC maximum.

At all stations the brassicasterol/cholesterol ratio for the small particle size fraction was the highest in the upper 100 m (Table 2). In the mesopelagic and deep ocean this ratio decreased systematically to reach a value close to 1. This condition reflected the relative variation of autotrophic organic material (brassicasterol) vs. heterotrophic material (cholesterol) contribution to the export flux of organic material with increasing depth. For large particles the brassicasterol to cholesterol ratio stayed close to 1 with very surface waters having slightly larger ratios than underlaying waters (Table 3). Such low values reflected larger contributions of hetetrotrophs vs. autotrophs in this large size fraction of particles compared to the smaller sized particles.

3.2 δ^{13}C composition of POC, cholesterol and brassicasterol

The vertical profiles for $\delta^{13}C_{LP-POC}$, $\delta^{13}C_{SP-POC}$, $\delta^{13}C_{SP-cholesterol}$ and $\delta^{13}C_{SP-brassicasterol}$ are shown in Figure 4 (all dataset in Tables 1 and 2). Note that for S1 and S2 SP-brassicasterol data are limited to the upper water column, since

Selected sterols and their δ^{13}C in the Southern Ocean water column

A.-J. Cavagna et al.

concentrations fell below detection limit deeper in the deeper water column. The range of δ^{13}C variation through the water column can reach up to 10‰ (see for example the $\delta^{13}C_{SP-cholesterol}$ profile at station S2; Fig. 4). At stations S1 and S2 δ^{13}C profiles of sterols and bulk POC do cross over at depth, while at stations S3 to S5 these are clearly separated from each other.

At S1 and to a lesser extent at S2, $\delta^{13}C_{LP-POC}$ values decreased below 2750 m and converge toward the $\delta^{13}C_{SP-POC}$ values (Table 2, Fig. 4). At these depths the water mass consisted of diluted North Atlantic Deep Water (NADW) from the eastern route (S. Speich, personal communication, 2009). This could be an indication of NADW transporting highly degraded organic matter constituted by isotopically light refractory lipidic material since it has been shown that proteins and carbohydrates (higher δ^{13}C isotopic signals than lipids, see Galimov, 2006) are more labile compared to lipids and are then removed preferentially from the particulate organic matter (POM) (Degens, 1969). Also, intense bacterial degradation of the more labile carbohydrates and proteins could explain this strong decrease in δ^{13}C-POC observed for large particles at S1 and S2. Stations S1 and S2 are defined by mixed phytoplanktonic community composed of dinoflagellates, chromophytes, nanoflagellates and cyanobacteria, and are defined as systems supported to a large degree by regenerated production (Joubert et al., this issue). Taking the time lag due to sinking speed into account, observed variations of $\delta^{13}C_{SP-POC}$ and $\delta^{13}C_{LP-POC}$ along the S1 and S2 depth profiles could indeed be linked to high degradation processes occurring in the surface water.

At S2 all δ^{13}C values in the upper 600 m decreased with depth, whereas below 600 m they increased (note that SP-brassicasterol was not detected below 600 m). Below 1500 m LP-$\delta^{13}C_{POC}$ decreased again, as observed at S1 (see above). At S3 below the surface waters $\delta^{13}C_{LP-POC}$ and $\delta^{13}C_{SP-cholesterol}$ showed a gradual increase with depth, while $\delta^{13}C_{SP-POC}$ and $\delta^{13}C_{SP-brassicasterol}$ remained rather unchanged over the entire water column (Fig. 4). At S4 within the upper 100 m $\delta^{13}C_{LP-POC}$ and $\delta^{13}C_{SP-brassicasterol}$ decreased with depth. At greater depth, $\delta^{13}C_{LP-POC}$ and

$\delta^{13}C_{SP-cholesterol}$ increased rather uniformly with depth while $\delta^{13}C_{SP-POC}$ barely changed with depth. $\delta^{13}C_{SP-brassicasterol}$ strongly increased from the surface water to 1000 m. At S5 all components showed a gradual $\delta^{13}C$ increase with depth (Fig. 4).

4 Discussion

Since this study presents the first complete depth profiles of $\delta^{13}C$ data on cholesterol and brassicasterol in the Southern Ocean from Cape Basin to the northern Weddell Gyre, we focus the discussion on the observed variation below the surface layers, with the aim of using these proxies to provide insight into the fate of organic matter sinking out of the surface water where the photosynthetic signal is acquired.

4.1 Variation of brassicasterol and cholesterol content with depth

The increase of SP-sterol contents relative to SP-POC and (Fig. 3, lower panel) in the mesopelagic layer (100 to 1000 m) overlaps with the domain of excess [234]Th activity and excess particulate Barium during the BONUS-GoodHope expedition, discussed by Planchon et al. (2012). In that paper it is reported that excess [234]Th and particulate Barium reflect the processes of particle break-up and organic matter remineralisation. The observation that in some cases the contribution of large particles to total POC (Fig. 3, upper panel) also increases in mesopelagic waters may reflect local zooplanktonic activity, possibly feeding on the vertical particle flux thereby synthesizing cholesterol. Our present data do confirm the significance of mesopelagic waters as a region where the flux of material exported from the surface undergoes major changes.

Figure 5a shows the depth variation of brassicasterol over cholesterol ratios (bra:cho) with depth (see also Table 2). Two clear trends emerge from these data: (i) first, bra:cho ratios are highly variable and mainly >1 in the upper 500 m waters (surface water and upper part of the mesopelagic layer); (ii) secondly, bra:cho ratios stabilize at values of ~1 in the lower 500 m waters (lower mesopelagic layer and deep water.

Furthermore, the lowest value of bra:cho (0.5 at station S2, 608 m; 0.4 at station S4, 749 m; Table 2) are observed at intermediate depths, between 500 and 1000 m. As already highlighted in the Results section, the general decrease of bra:cho ratios reflects the relative decrease of autotrophic organic material (brassicasterol - phytoplankton)

5 vs. heterotrophic material (cholesterol - zooplankton) with increasing depth and its stabilization around 1 in the deep water. These observations lead to the hypothesis that the role of zooplankton in the carbon export composition increases with depth compared to the surface water and shows a maximum role between 500 and 1000 m in the mesopelagic layer. Deeper, the bra:cho ≈ 1 is probably due to an equilibrium

10 reached between the 2 components and their most refractory fraction below the twilight zone where most of the attenuation of the carbon export flux occurs.

To evaluate the importance of such processes at different depth layers we propose in Fig. 6 (panel B is a zoom of panel A) the linear regressions obtained from the correlation between bra and cho concentrations, taking into account that the entire dataset can

15 be split in two groups (group A from surface to 500 m, group B from 500 m to the deep ocean). We obtain a general image for the BONUS-GoodHope transect covering 5 complete water column sampling stations located in five different Southern Ocean regions (see Sect. 2.1.). Regression slopes are 0.5 ± 0.1 (p-value < 0.05) and 1.5 ± 0.2 (p-value < 0.05) for the upper 500 m and the water column below 500 m, respectively.

20 Our results suggest that in the upper 500 m the major contributor to the sterol pool is phytoplankton, whereas between 500 and 1000 m it becomes zooplankton. Finally, these two components reach stable proportions below 1000 m depth. These results suggest a key role of faecal aggregates in routing carbon to the deep ocean, as highlighted by Ebersbach et al. (2011) for the Australian sector of the Southern Ocean.

25 However, further data would be of great interest to enlarge the resulting observations for the case of BONUS-GoodHope transect.

4.2 Variation of δ^{13}C signatures with depth

We observed that in general the $\delta^{13}C_{SP-sterols}$ but also $\delta^{13}C_{LP-POC}$ (S1, S2 excepted; see above Sect. part 3.2. and Fig. 4) increase with depth, whereas $\delta^{13}C_{SP-POC}$ remains stable throughout the water column profile. Figure 5b shows depth variations of calculated values of $\varepsilon_{cholesterol}$ and $\varepsilon_{brassicasterol}$ for the complete dataset. This ε is based on a simple calculation (ε_{sterol} (‰) = $\delta^{13}C_{SP-sterol} - \delta^{13}C_{SP-POC}$) allowing us to estimate the apparent offset between the ^{13}C isotopic signal of SP-POC and studied sterols. Indeed $\varepsilon_{brassicasterol}$ ranges between −13.6‰ and −4.1‰ in the upper 500 m and then stabilizes around −7‰ below 500 m. On the other hand, $\varepsilon_{cholesterol}$ shows a pronounced increase from the surface water ($\varepsilon_{cholesterol}$ ranges between -12.3‰ and −5.2‰) to the deep ocean where it reaches a value of ∼ +5‰. The stabilization of $\varepsilon_{brassicasterol}$ around -7‰ below 500 m is in accordance with previous laboratory experiments estimating a ε_{sterol} of −7‰ (Bidigare et al., 1997; Schouten et al., 1998; see also Popp et al., 1999 for an application to Southern ocean surface water data analysis). However, previous studies were performed for laboratory experiments on growth rate of various phytoplankton groups or surface water samples, while the present observation concerns samples below the euphotic layer where no more biosynthesis of brassicasterol is possible since it is only synthesized by phytoplankton. However, we previously observed that $\delta^{13}C_{SP-POC}$ is stable through the entire water column, and thus hypothesize that the stable $\varepsilon_{brassicasterol}$ of −7‰ below 500m indicates that this sterol is biosynthesized in the surface water and not below. On the other hand, the increase of $\varepsilon_{cholesterol}$ with depth could reflect several factors which will be described below.

Although it can not be excluded that the observed increase of δ^{13}C-cholesterol is partly due to the Suess effect reflecting the invasion of the upper ocean by isotopically light anthropogenic CO_2 reflected till the secondary producers, this would imply a large age difference between deep and surface ocean suspended matter (the former much older than the latter; Suess, 1980). Considering particle sinking velocities between

50 and 150 m per day (McDonnell and Buesseler, 2010) it is evident that the time lag between the bloom events that generate the deep ocean particles and those that generate the particles in the upper layers is much inferior to the period covering the bulk of the anthropogenic CO_2 emissions (weeks, months vs. years). Therefore, it is probable that the observed lower δ^{13}C values for surface ocean SP-sterols compared to deep ocean values are due to factors other than the Suess effect. Below, we discuss several possible mechanisms leading to isotopically heavier organic carbon and also sterols.

4.2.1 Growth rate related effect

Fry and Wainright (1991) report that fast-growing diatoms are ^{13}C-enriched compared to more slowly growing cells. Highest growth rates occur during the early season when there is no nutrient limitation, while later in the season growth rates decrease due to the onset of nutrient limitation conditions (see e.g. Arrigo, 2002), the latter leading to more pronounced isotope fractionation and thus more ^{13}C-depleted phytoplankton (e.g., Popp et al., 1999). During the end of the growing season, we would thus expect relatively ^{13}C-depleted phytoplankton in the upper water column, while the ^{13}C-enriched cells from the start of the growing season would have reached the deeper water column. Such mechanism could explain the observed enrichment in $\delta^{13}C_{cholesterol}$ with depth in the case of BONUS-GoodHope, which took place during the austral summer, i.e., the end of the productive season.

4.2.2 Particle size related effects

Pancost et al. (1997) report a particle size-dependency for $\delta^{13}C_{brassicasterol}$, with a ^{13}C enrichment in suspended particles >20 μm relative to the <20 μm fraction. This suggests that surface-area to volume ratios control the fractionation of carbon isotopes by diatoms, as confirmed by Popp et al. (1998). Therefore, a relatively increased contribution of larger phytoplankton to the export flux could explain the observed δ^{13}C

enrichment with depth. Selective feeding of zooplankton on larger cells and active transport of this material to deeper layers during migration (Steinberg et al., 2008) might cause the translocation of isotopically heavier material to deeper waters, while leaving isotopically lighter material -associated with smaller particles- in the surface
5 layers.

4.2.3 Sea-ice algae related effect

A further possible process leading to ^{13}C-enriched organic material is related to the activity of phytoplankton thriving in sea-ice brines. Sea-ice phytoplankton is significantly enriched in ^{13}C compared to pelagic phytoplankton in adjacent open waters because
10 of carbon limitation in the brine pockets and due to physiological properties such as the presence of carbon concentrating mechanisms and/or the uptake of bicarbonate (HCO_3^-) (Gleitz et al., 1996; Gibson et al., 1999; Villinski et al., 2000). Melting of sea-ice with release of sea-ice phytoplankton occurs during the growth season, so these isotopically heavy particles, if sinking out of the surface waters, can be expected to
15 be found deeper in the water column. For the most southern stations (S4, S5), which are influenced by the Seasonal Ice Zone (SIZ) in winter, sinking of sea-ice algae could contribute to ^{13}C enrichment of organic C at depth.

4.2.4 Other processes potentially affecting variations of $\delta^{13}C_{POC}$

Several further processes different from those listed above could affect the isotopic
20 composition of deep ocean POC. These processes include: (i) preferential degradation of the more labile carbohydrate and protein material which is ^{13}C-enriched compared to lipids (Degens, 1969; Galimov, 2006); (ii) ^{13}C enrichment of sinking particles due to selective grazing on the larger ^{13}C-enriched cells (see discussion above) followed by fecal pellet production; (iii) loss of ^{13}C-depleted carbon associated with methane
25 production by prokaryotes within zooplankton digestive tracts (Freeman, 2001; Hayes, 1993); (iv) increase in the contribution of heterotrophic POC to the total POC pool, due

to transfer of organic carbon to higher trophic levels (∼1–2‰ enrichment per increasing trophic level due to respiratory effects; DeNiro and Epstein, 1978; Fry, 1988; Fry and Sherr, 1984).

We note, however, that $\delta^{13}C_{SP-POC}$ did not show an increase with depth. We hypothesize that in this case there may be a balance between a $\delta^{13}C_{SP-POC}$ decrease due to preferential loss of ^{13}C-enriched, more labile carbon phases (carbohydrates, proteins; see above) and a $\delta^{13}C_{SP-POC}$ increase due to the trophic level succession effect, inducing an increase ∼1–2‰ keeping $\delta^{13}C_{SP-POC}$ rather unchanged through the deep water column. Alternatively, it might simply be that small particles are indeed representative of organic matter biosynthesized in the surface water. This would imply then a fast transfer mechanism for these particles. Recent work by McDonnell and Buesseler (2010) did reveal that sinking velocity is largest not only for the largest particles they studied (up to 1 mm), but also for the small sized particles (<50 µm). Clearly, any realistic scenario for ^{13}C enrichment of biomarkers with depth needs also to comply with the observation that POC of the <53 µm size class does not show a significant ^{13}C enrichment with depth.

In summary, the observed isotopic increase for SP-cholesterol with depth would need a cell size or growth rate related impact on isotopic fractionation and a mechanism separating isotopically heavy from light cells. This mechanism could be (1) a separation in time between sinking of isotopically heavier cells (early season) and light cells (late season) and/or (2) selective zooplankton grazing on larger isotopically heavier cells and their transfer to the deep sea via fecal pellets. The first hypothesis implies an age difference between deep and surface particles, while the second one does not. However, the absence of a significant δ^{13}C variation of SP-POC with depth requires that the above processes affecting $\delta^{13}C_{SP-cholesterol}$ are somehow neutralized for SP-POC (via a balance between preferential degradation of isotopically heavy compounds such as carbohydrates and proteins and isotopic enrichment due to trophic translocation of organic matter).

As an additional hypothesis, we also stress a possible effect of high pressure on cholesterol biosynthesis occurring below the surface water: cholesterol is a component of cell membrane and the idea is that ^{13}C-^{13}C covalent bond is stronger than ^{12}C-^{12}C covalent bond. Such specificity could be of great interest to resist high pressure effect and would imply an increase of $\delta^{13}C_{cholesterol}$ with depth.

Our observations stress the interest of studying both $\delta^{13}C_{POC}$ and $\delta^{13}C_{sterol}$ in sinking and suspended particles since it allows gaining information on the fate of organic matter in the whole water column via cross-comparison.

4.3 Variation of whole water column $\delta^{13}C$ signatures with [CO$_2$]$_{aq}$.

Figure 7 shows the latitudinal variation of $\delta^{13}C_{LP-POC}$ (Fig. 7a), $\delta^{13}C_{SP-POC}$ (Fig. 7b), $\delta^{13}C_{SP-cholesterol}$ (Fig. 7c), $\delta^{13}C_{SP-brassicasterol}$ (Fig. 7d) vs. surface CO_{2aq} concentration (μmol kg^{-1}) (from Gonzáles-Dávila et al., 2011) for the arbitrarily defined surface water (0–100 m), mesopelagic layer (100–1000 m), deep ocean (>1000 m) and bottom waters. In parallel, we obtain a good correlation between $\delta^{13}C_{SP-brassicasterol}$ and $\delta^{13}C_{SP-cholesterol}$ all dataset ($\delta^{13}C_{SP-cholesterol} = (0.7 \times \delta^{13}C_{SP-cholesterol}) - 8.0$; $R^2 = 0.8$; not shown).

For the global ocean (Goericke and Fry, 1994) and the Southern Ocean (Lourey et al., 2004; O'Leary et al., 2001; Popp et al., 1999; Dehairs et al., 1997), a number of studies highlight a close inverse relationship between sea surface temperature (SST), CO_2 aq. and $\delta^{13}C_{POC}$. François et al. (1993) demonstrate using models from O'Leary (1981) and Farquhar et al. (1982), that the carbon isotopic composition of phytoplankton is primarily determined by (i) the isotopic composition of the source of inorganic carbon; (ii) the isotopic fractionation during transport into and out of the cell; (iii) isotopic discrimination during carboxylation and the degree of leakage of intracellular inorganic carbon. When focus is on the isotopic composition of the source (marine algae take up either CO_2 aq. or bicarbonate HCO_3^-, or both), François et al. (1993) stress that δ^{13}C-bicarbonate varies little from warm to cold surface water ($\sim$ +1 to +2‰; Kroopnick,

1985) and in case phytoplankton incorporate bicarbonate it would tend to increase $\delta^{13}C_{POC}$. In contrast, $\delta^{13}C_{CO_2\ aq.}$ systematically decreases from $\sim$−7.5‰ in warm water to $\sim$ -10‰ in cold Southern Ocean surface water. François et al. (1993) conclude that changes in the isotopic composition of CO_2 aq. can contribute significantly to the observed latitudinal trend in $\delta^{13}C_{POC}$ (a circa 2.5‰ decrease contribution). For $\delta^{13}C_{sterols}$ in surface water Popp et al. (1999) and Tolosa et al. (1999) demonstrate a similar behavior than for $\delta^{13}C_{POC}$ in Southern Ocean and in Indian Ocean surface waters, respectively.

Several factors such as substrate concentration, growth rate, cell geometry, plankton species, and nutrient availability reviewed in François et al. (1993) and Popp et al. (1999) may account for the covariance between $\delta^{13}C$ of phytoplankton or specific compounds and CO_2 aq., and for the differences between regressions for the different C pools. However, the good correlation between $\delta^{13}C_{SP-brassicasterol}$ and $\delta^{13}C_{SP-cholesterol}$ all dataset (see above) mainly reflects the key role of change in the isotopic composition of CO_2 aq. with latitude.

4.3.1 Surface water variations

$\delta^{13}C_{LP-POC}$ and $\delta^{13}C_{SP-POC}$ values decrease from −21.2 ± 0.7 (S1, 36°31'S) to −29.4 ± 0.5‰ (S5, 57°33' S) and from −20.9 ± 0.1 (S1) to −28.7 ± 0.2‰ (S5), respectively (Fig. 7a, b; Tables 4, 5). In contrast, CO_2 aq. concentrations increase between 36° S and 57° S from 10.7 ± 0.3 µmol kg^{-1} to 24.0 ± 0.3 µmol kg^{-1} (Table 5, Gonzáles-Dávila et al., 2011). This results in significant inverse correlations between $\delta^{13}C_{POC}$ and surface CO_2 aq.. The $\delta^{13}C$ decrease is similar between small and large particles reaching on average 8.0 ± 0.2‰ from S1 to S5 (from Table 4). Such a decrease is similar to what has been reported by Goericke and Fry (1994) for Southern Ocean waters, but larger than the value of approximately 5‰ reported by François et al. (1993).

As observed for $\delta^{13}C_{POC}$, the decrease in $\delta^{13}C_{LP\ and\ SP-cholesterol}$, and $\delta^{13}C_{LP\ and\ SP-brassicasterol}$ in the surface water coincides with an increase in CO_2 aq.

content (Table 4). However, the average (LP and SP) decrease reaches –11.1 ± 1.9‰ and –14.7 ± 0.9‰ for cholesterol and brassicasterol, respectively (from Table 4), which is larger than for small and large particle POC. This observation is in agreement with Popp et al. (1999) who report that the individual sterol isotopic compositions in surface waters (WOCE SR3 transect, 145° E, between 45°55′ S to 65°24′ S) generally decrease southward and exceed the variations in bulk δ^{13}C$_{POC}$.

Our data reveal for large particles that the difference in δ^{13}C composition between LP-POC and LP-cholesterol is between –6.0 and –10.3‰ (Table 4), while the difference between LP-POC and LP-brassicasterol δ^{13}C ranges between –6.8 and –13.9‰. For small particles the difference between POC and cholesterol ranges between –6.2 to –9.3‰ and the difference between POC and brassicasterol between –5.8 to –10.9‰. Such offsets appear to increase southward. Tolosa et al. (1999) estimate the δ^{13}C isotopic difference between bulk organic matter and cholesterol to be 5‰, and stress that such difference is typically observed between whole plant material and extractable lipids (Hayes, 1993). While for the northern part of the BGH transect our data are close to the observations of Tolosa et al. (1999), in general we observe a larger δ^{13}C difference between POC and cholesterol, and the discrepancy is enhanced southward. This enhanced discrepancy could be related to larger cells contribution (diatoms).

4.3.2 Mesopelagic and deep ocean

For the δ^{13}C$_{LP-POC}$ regressions against CO$_{2aq.}$ the slopes are quite variable (Fig. 7a, Table 5) without a clear trend with depth. On the other hand, the slopes of the δ^{13}C$_{SP-POC}$ vs. CO$_{2aq.}$ regressions are quite conservative throughout the water column (Fig. 7b, Table 5). Thus, observations of δ^{13}C$_{SP-POC}$ signal conservation with depth suggest that this proxy would be useful for paleoclimatology. On the other hand, this proxy is confirmed as useless to trace fate of organic matter in the whole water column on its own since it shows stable signal from the surface to the deep ocean.

While the slopes of the regressions of $\delta^{13}C_{SP-cholesterol}$ vs. CO_2 aq. are significantly conserved with depth (Fig. 7c, Table 5), the regression intercepts do evolve with depth revealing a tendency for higher $\delta^{13}C_{cholesterol}$ values in the deep ocean and in proximity of the seafloor (see Sect. 4.2.1 and 4.2.2. for hypothetical explanation). $\delta^{13}C_{SP-brassicasterol}$ shows a significant decrease of regression slopes between surface and deep ocean and from the north to the south part of the Southern Ocean (Fig. 7d, Table 5). It is not unlikely (though not confirmed here) that this reflects an enhanced contribution of sea-ice diatoms south of the BGH transect (S4 and S5, see above Sect. 4.2.3.), although this cannot be unambiguously demonstrated by our data. These two proxies appear thus useful to trace fate of organic matter in the whole water column.

5 Conclusions

Although the BONUS-GoodHope transect crossed several frontal structures and specific biogeochemical zones, our study showed several general patterns in brassicasterol and cholesterol concentrations, bra:cho ratios, and δ^{13}C signatures of POC, cholesterol and brassicasterol along depth and latitudinal gradients. First, the bra:cho ratio, which reflects the relative importance of autotrophs vs. heterotrophs, shows a general trend relevant for each of the five studied stations: in the upper 500 m depth the major component of organic material is phytoplankton (bra:cho ratios highly variable and >1) , whereas between 500 and 1000 m depth the major component becomes zooplankton (bra:cho ratios reaching values <1 in the mesopelagic layer). Finally, these two components reach stable ratio below 1000 m depth (bra:cho ~1). Our observations support a key role of fecal aggregates in the fate of organic matter and export to deep ocean.

Second, depth variation of $\varepsilon_{brassicasterol}$ and $\varepsilon_{\ cholesterol}$ shows again general trends valuable for the five stations. This indeed highlights (i) that brassicasterol is only biosynthesized in the surface water; thus showing a stable value close -7‰ below 500 m depth in accordance with Schouten et al. (1998) and Bidigare et al. (1997); (ii) an

increase of $\varepsilon_{\text{cholesterol}}$ with depth which is mainly defined to be related to growth rate related effect and/or particle size related effect and selective feeding by zooplankton. A role of sea-ice algae release south of the transect is also proposed to act on latitudinal and depth variations of $\delta^{13}C_{\text{brassicasterol}}$ and $\delta^{13}C_{\text{cholesterol}}$. As an additional hypothesis,

5   we also suggest that a high pressure effect on cholesterol biosynthesis below the surface water might induce an increase of $\delta^{13}C_{\text{cholesterol}}$ in deeper waters.

     Third, the relationship between $CO_{2\text{aq.}}$ concentration and $\delta^{13}C_{\text{SP−sterols}}$ is generally maintained throughout the deep ocean. This observation was not expected a priori, since circulation of deep waters carrying suspended matter formed in different regions

10   may possibly dilute the isotopic signatures resulting from biological activity in local surface waters. It thus seems that export of organic matter and fate of organic compounds in the deep sea closely fit to a 1D scheme (surface to deep ocean). In case further studies confirm this observation, the fact that regressions of $\delta^{13}C_{\text{cholesterol}}$ and $\delta^{13}C_{\text{SP−POC}}$ versus $CO_{2\text{aq.}}$ are quite conservative with depth highlights the potential of

15   these proxies for surface water CO_2 aq. concentration. Future field work is necessary to confirm variability and trends observed during this study, and to adequately constrain the application of such this potential proxy.

     While not conclusive, this first dataset on combined $\delta^{13}C$ and concentrations measurements of both bulk organic C and specific sterol markers throughout the water

20   column shows the promising potential of analyzing $\delta^{13}C$ signatures of individual marine sterols to explore the recent history of plankton and the fate of organic matter in the SO.

References

Arístegui, J., Agusti, S., Middelburg, J. J., and Duarte, C. M.: Respiration in the mesopelagic and bathypelagic zones of the ocean, Respiration in Aquatic Ecosystems, 181, 2005.

Arrigo, K.: Marine microorganisms and global nutrient cycles, Nature, 437, 349–355, 2002.

Battle, M., Bender, M. L., Tans, P. P., White, J. W. C., Ellis, J. T., Conway, T., and Francey, R. J.: Global carbon sinks and their variability inferred from atmospheric O_2 and $\delta^{13}C$, Science, 287, 2467–2470, 2000.

Bentaleb, I., Fontugne, M., Descolas-Gros, C., Girardin, C., Mariotti, A., Pierre, C., Brunet, C., and Poisson, A.: Carbon isotopic fractionation by plankton in the Southern Indian Ocean, J. Marine Syst., 17, 39–58, 1998.

Bidigare, R. R., Fluegge, A., Freeman, K. H., Hanson, K. L., Hayes, J. M., Hollander, D., Jasper, J. P., King, L. L., Laws, E. A., Milder, J., Millero, F. J., Pancost, R., Popp, B. N., Steinberg, P. A., and Wakeham, S. G.: Consistent fractionation of ^{13}C in nature and in the laboratory: Growth-rate effects in some haptophyte algae, Global Biogeochem. Cy., 11, 279–292, 1997.

Bligh, E. G. and Dyer, W. J.: A rapid method of total lipid extraction and purification, Can. J. Biochem. Physiol., 31, 911–917, 1959.

Boschker, H. T. S.: Linking microbial community structure and functioning: stable isotope (13C) labeling in combination with PLFA analysis, 1673–1688, in: Molecular Microbial Ecology Manual II, edited by: Kowalchuk, G. A., de Bruijn, F. J., Head, I. M., Akkermans, A. D., and van Elsas, J. D., Kluwer Academic Publishers, Dordrecht, The Netherlands, 2004.

Boyd, P. W. and Trull, T. W.: Understanding the export of biogenic particles in oceanic waters: Is there a consensus? Progress in Oceanography, 72, 276–312, 2007.

Burd, A. B., Hansell, D. A., Steinberg, D. K., Anderson, T. R., Arístegui, J., Baltar, F., Beaupré, S. R., Buesseler, K. O., Dehairs, F., Jackson, G. A., Kadko, D. C., Koppelmann, R., Lampitt, R. S., Nagata, T., Reinthaler, T., Robinson, C., Robison, B. H., Tamburini, C., and Tanaka, T.: Assessing the Apparent Imbalance between Geochemical and Biochemical Indicators of Meso- and Bathypelagic Biological Activity: What the @$#! is wrong with present calculations of carbon budgets? Deep-Sea Res. Pt. II, 57, 1557–1571, 2010.

Chikarahishi, Y.: Carbon and hydrogen isotopic composition of sterols in natural marine brown and red macroalgae and associated shellfish, Organic Geochemistry, 37, 428–436, 2006.

Degens, E.: Biogeochemistry of stable isotopes, in: Organic Geochemistry, edited by: Eglinton, G., Murphy, M. T. J., Springer, Heidelberg, New York, 304–329, 1969.

Selected sterols and their $\delta^{13}C$ in the Southern Ocean water column

A.-J. Cavagna et al.

Title Page

Abstract | Introduction

Conclusions | References

Tables | Figures

◄ | ►

◄ | ►

Back | Close

Full Screen / Esc

Printer-friendly Version

Interactive Discussion

DeNiro, M. J. and Epstein, S.: Influence of diet on the distribution of carbon isotopesin animals, Geochimica et Cosmochimica Acta, 42, 495–506, 1978.

Dehairs, F., Kopczynska, E., Nielsen, P., Lancelot, D., Bakker, D. C. E., Koeve, W., and Goeyens, L.: δ^{13}C of Southern Ocean suspended organic matter during spring and early summer: regional and temporal variability, Deep-Sea Res. Pt. II, 44, 129–142, 1997.

Ebersbach, F., Trull, T. W., Davies, D. M., and Bray, S. G.: Controls on mesopelagic particle fluxes in the Sub-Antarctic and Polar Frontal Zones in the Southern Ocean south of Australia in summer - Perspectives from free-drifting sediment traps, Deep-Sea Res. Pt. II, 58, 2260–2276, 2011.

Farquhar, G. D., O'Leary, M. H., and Berry, J. A.: On the relationship between carbon isotope discrimination and the intercellular carbon dioxide concentration in leaves, Australian J. Plant Physiol., 9, 121–137, 1982.

François, R., Altabet, M. A., Goericke, R., McCorckle, D. C., Brunet, C., and Poisson, A.: Changes in the δ^{13}C of surface water particulate organic carbon across the Subtropical Convergence in the SW Indian Ocean, Global Biogeochem. Cy., 7, 627–644, 1993.

Freeman, K. H.: Isotopic biogeochemistry of marine organic carbon, in: Stable isotopes geochemistry, reviews in mineralogy and geochemistry, vol. 43, edited by: Valley, J. W. and Cole, D. R., Mineralogy Society of America, Washington D.C, 579–605, 2001.

Fry, B.: Food web structures on Georges Banks from stable C, N and S isotopic compositions, Limnol. Oceanogr., 33, 1182–1190, 1988.

Fry, B. and Sherr, E.: δ^{13}C measurements as indicators of carbon flow in marine and freshwater ecosystems, Contr. Mar. Sci., 27, 13–47, 1984.

Fry, B. and Wainright, S. C.: Diatom sources of 13C-rich carbon in marine food webs, Mar. Ecol.-Prog. Ser., 76, 149–157, 1991.

Galimov, E. M.: Isotope Organic Geochemistry, Org. Geochem., 37, 1200–1262, 2006.

Gibson, J. A. E., Trull, T. W., Nichols, P. D., Summons, R. E., and McMinn, A.: Sedimentation of C-13 rich organic matter from Antarctic sea-ice algae: a potential indicator of sea-ice extent, Geology, 27, 331–334, 1999.

Gleitz, M., Kukert, H., Riebesell, U., and Dickmann, G. S.: Carbon acquisition and growth of Antarctic sea ice diatoms in closed bottle incubations, Mar. Ecol. Prog. Series, 135, 167–177, 1996.

Gonzáles-Dávila, M., Santana-Casiano, J. M., Fine, R. A., Happell, J., Delille, B., and Speich, S.: Carbonate system in the water masses of the Southeast Atlantic sector of the Southern

Selected sterols and their δ^{13}C in the Southern Ocean water column

A.-J. Cavagna et al.

Title Page

Abstract	Introduction
Conclusions	References
Tables	Figures

◄ | ►|

◄ | ►

Back | Close

Full Screen / Esc

Printer-friendly Version

Interactive Discussion

Ocean during February and March 2008, Biogeosciences, 8, 1401–1413, doi:10.5194/bg-8-1401-2011, 2011.

Grice, K., Klein Breteler, W. C. M., Schouten, S., Grossi, V., de Leeuw, J. W., and Sinninghe Damsté, J. S.: The effect of zooplankton herbivory on biomarker proxy records, Paleo-ceanography, 13, 686–693, 1998.

Goad, L. J. and Akihisa, T.: Analysis of sterols, Blackie Academic & Professional, 437 pp., 1997.

Goericke, R. and Fry, B.: Variations of marine plankton δ^{13}C with latitude, temperature, and dissolved CO_2 in the world ocean, Glob. Biogeochem. Cy., 8, 85–90, 1994.

Gordon, A. L.: Interocean exchange of thermocline water, J. Geophys. Res., 91, 5037–5046, 1986.

Gordon, A. L.: Oceanography: The brawniest retroflection, Nature, 421, 904–905, 2003.

Hayes, J. M.: Factors controlling ^{13}C contents of sedimentary organic compounds: Principle, 1993.

Honjo, S., Manganini, S. J., Krieshfield, S. A., and François, R.: Particulate organic carbon fluxes to the ocean interior and factors controlling the biological pump: A synthesis of global sediment trap programs since 1983, Prog. Oceanogr., 76, 217–285, 2008.

Joubert, W. R., Thomalla, S. J., Waldron, H. N., Lucas, M. I., Boyé, M., Le Moigne, F. A. C., Planchon, F., and Speich, S.: Nitrogen uptake by phytoplankton in the Atlantic sector of the Southern Ocean during late austral summer, Biogeosciences, 8, 2947–2959, doi:10.5194/bg-8-2947-2011, 2011.

Kennedy, H. and Robertson, J.: Variations in the isotopic composition of particulate organic carbon in surface waters along an 88°W transect from 67° S to 54°S, Deep-Sea Res. Pt. II, 42, 1109–1122, 1995.

Kroopnick, P. M.: The distribution of C-13 of TCO_2 in the world oceans, Deep-Sea Res., 32, 57–84, 1985.

Lagarda, M. J., García-Llatas, G., and Farré, R.: Analysis of phytosterols in foods, J. Pharmaceut. Biomed., 41, 1486–1496, 2006.

Le Moigne, F. A. C., Boyé, M., Masson, A., Corvaisier, R., Grosstefan, E., Guéneugues, A., Pondaven, P., and Nelson, D.: Biogeochemical features of the subtropical southeastern Atlantic and the Southern Ocean south of South Africa during the austral summer of the International Polar Year, Biogeosciences Discuss., in review, 2012.

Lorrain, A., Savoye, N., Chauvaud, L., Paulet, Y.-M., and Naulet, N.: Decarbonation and preser-

vation method for the analysis of organic C and N contents and stable isotope ratios of low-carbonated suspended particulate material, Anal. Chim. Acta, 491, 125–133, 2003.

Lourey, M. J., Trull, T. W., and Tilbrook, B.: Sensitivity of δ^{13}C of Southern Ocean suspended and sinking organic matter to temperature, nutrient utilization, and atmospheric CO_2, Deep-Sea Res. Pt. I, 51, 281–305, 2004.

Lutjeharms, J.: The Agulhas Current, 329 pp., Springer, Berlin, 2006.

McDonnell, A. M. P. and Buesseler, K. O.: Variability in the average sinking velocity of marine particles, Limnol. Oceanogr., 55, 2085–2096, 2010.

O'Leary, T., Trull, T. W., Griffiths, F. B., Tilbrook, B., and Revill, A. T.: Euphotic zone variations in bulk and compound-specific δ^{13}C of suspended organic matter in the subantarctic ocean, south of Australia, J. Geophys. Res., 106, 31669–31684, 2001.

O'Leary, M. H.: Carbon isotope fractionation in plants, Phytochem., 20, 553–567, 1981.

Pancost, R. D., Freeman, K. H., Wakeham, S. G., and Robertson, C. Y.: Control on carbon isotopic fractionation by diatoms in the Peru upwelling region, Geochim. Cosmochim. Acta, 61, 4983–4991, 1997.

Planchon, F., Cavagna, A.-J., Cardinal, D., André, L., and Dehairs, F.: Late summer particulate organic carbon export from mixed layer to mesopelagic twilight zone in the Atlantic sector of Southern Ocean, Biogeosciences Discuss., in preparation, 2012.

Popp, B. N., Laws, E. A., Bidigare, R. R., Dore, J. E., Hanson, K. L., and Wakeham, S. G.: Effect of phytoplankton cell geometry on carbon isotopic fractionation, Geochim. Cosmochim. Acta, 62, 69–77, 1998.

Popp, B. N., Trull, T. W., Kenig, F., Wakeham, S. G., Rust, T. M., Tilbrook, B., Griffiths, F. B., Wright, S. W., Marchant, H. J., Bidigare, R. R., and Laws, E. A.: Control on the carbon isotopic composition of Southern Ocean phytoplankton, Global Biogeochem. Cy., 13, 827–844, 1999.

Ralston, D., Mcgillicuddy, jr D. J., and Townsend, D. W.: Asynchronous vertical migration and bimodal distribution of motile phytoplankton, J. Plankton Res., 29, 803–821, 2007.

Rampen, S. W., Abbas, B. A., Schouten, S., and Sinninghe Damsté, J. S.: A comprehensive study of sterols in marine diatoms (Bacillariophyta): Implications for their use as tracers for diatoms productivity, Limnol. Oceanogr., 55, 91–105, 2010.

Rau, G. H., Riebesell, U., and Wolf-Gladrow, D.: CO_2 aq-dependent photosynthetic ^{13}C fractionation in the ocean: a model versus measurements, Global Biogeochem. Cy., 11, 267–278, 1997.

Reinthaler, T., van Aken, H., Veth, C., Arístegui, J., Robinson, C., Williams, P. J. B., Lebaron, P., and Herndl, G. J.: Prokaryotic respiration and production in the meso- and bathypelagic realm of the eastern and western North Atlantic basin, Limnol. Oceanogr., 51, 1262–1273, 2006.

Schouten, S., Klein Breteler, W. M. C., Blokker, P., Schogt, N., Rijpstra, W. I. C., Grice, K., Baas, M., and Sinninghe Damsté, J. S.: Biosynthetic effects on stable carbon isotopic compositions of algal lipids: Implications for deciphering the carbon isotopic biomarker record, Geochem. Cosmochim. Acta, 62, 1397–1406, 1998.

Steinberg, D. K., Van Mooy, B. A. S., Buesseler, K. K., Boyd, P. W., Kobari, T., and Karl, D. M.: Bacterial vs. zooplankton control of sinking particle flux in the ocean's twilight zone, Limnol. Oceanogr., 53, 1327–1338, 2008.

Suess, E.: Particulate organic carbon flux in the oceans - surface productivity and oxygen utilization, Nature, 288, 260–263, 1980.

Tolosa, I., Lopez, J. F., Bentaleb, I., Fontugne, M., and Grimalt, J. O.: Carbon isotope ratio monitoring-gas chromatography mass spectrometric measurements in the marine environment: biomarker sources and paleoclimate applications, The Science of Total Environment, 237/238, 473–481, 1999.

Trull, T. W. and Armand, L.: Insights into Southern Ocean carbon export from the δ13C of particles and dissolved inorganic carbon during the SOIREE iron release experiment, Deep-Sea Res. Pt. II, 11/12, 2655–2680, 2001.

Villinski, J. C., Dunbar, R. B., and Mucciarone, D. A.: Carbon-13 Carbon-12 ratios of sedimentary organic matter from the Ross Sea, Antarctica: a record of phytoplankton bloom dynamics, J. Geophys. Res.-Oceans, 105, 14163–14172, 2000.

Volkman, J. K.: A review of sterol markers for marine and terrigenous organic matter, Org. Geochem., 9, 83–99, 1986.

Volkman, J. K.: Sterols in microorganisms, Appl. Microbiol. Biotechnol., 60, 495–506, doi:10.1007/s00253-002-1172-8, 2003.

Wakeham, S. G., Lee, C., Peterson, M. L., Liu, Z., Szlosek, J., Putnam, I. F., and Xue, J.: Organic biomarkers in the twilight zone - Time series and settling velocity sediment traps during MedFlux, Deep-Sea Res. Pt. II, 56, 1437–1453, 2009.

Title Page

Abstract | Introduction

Conclusions | References

Tables | Figures

◄ | ►|

◄ | ►

Back | Close

Full Screen / Esc

Printer-friendly Version

Interactive Discussion

Selected sterols and their δ^{13}C in the Southern Ocean water column

A.-J. Cavagna et al.

Table 1. $\delta^{13}C_{POC}$ (‰) and POC concentration (µg l^{-1}) for large (>53 µm) and small (53 >> 1 µm) particles. Standard error on δ^{13}C measurements is the analytical standard deviation ($\sigma_{SD} = \pm 0.10$‰). N. D. means no data.

	depth	density	large particles δ^{13}C-POC	POC	small particles δ^{13}C-POC	POC	% large vs. total
	(m)	(g L^{-1})	(‰)	(µg l^{-1})	(‰)	(µg l^{-1})	(large + small)
station S1							
36°31′ S	50	1025.9	−20.8	1.6	−20.9	11.8	11.8
13°07E	75	1026.4	−21.7	1.0	N.D.	N.D.	
	125	1026.9	−21.5	0.2	−22.5	11.3	1.8
	175	1027.4	−23.5	0.0	N.D.	N.D.	
	250	1027.7	−22.6	0.1	−21.1	2.9	4.1
	500	1029.2	−18.1	0.1	−21.6	2.1	3.7
	750	1030.5	−19.7	0.1	−21.8	2.1	5.4
	1250	1033.3	N.D.	N.D.	−21.2	1.0	
	2750	1040.3	−15.7	0.0	−26.8	2.6	0.8
	4700	1049	−25.3	0.1	−26.4	3.5	2.7
station S2							
42°28′ S	30	1026.2	−19.7	4.6	−21.6	38.6	10.6
08°55′ S	75	1026.7	−20.5	1.6	−22.3	21.2	7.0
	130	1027.2	−21.7	0.3	−22.3	5.3	4.7
	250	1028	−21.9	0.4	−23.2	4.3	7.8
	590	1029.8	−21.6	0.0	−24.7	1.2	3.9
	608	1030.1	−21.8	0.2	−24.8	2.7	7.9
	1450	1034.4	−16.9	0.0	−21.9	1.2	2.6
	2900	1041	−25.1	0.1	−23.1	0.7	12.4
	2910	1041.1	−19.4	0.0	−23.6	0.6	3.6
	3940	1045.7	−26.0	0.1	−21.9	0.8	12.3
station S3							
47°33′ S	20	1026.6	−25.4	2.9	−25.0	39.9	6.8
04°22′ S	50	1026.7	−25.2	1.1	−24.9	39.6	2.7
	150	1027.6	−24.9	0.7	−23.8	5.0	12.8
	230	1028.2	−24.5	0.1	−22.8	3.9	2.6
	450	1029.5	−23.5	0.9	−23.5	2.4	27.0
	550	1030	−23.2	0.9	−23.8	2.8	24.2
	1060	1032.5	−23.0	0.1	−24.9	2.1	5.4
	1088	1032.6	−23.9	0.3	−24.0	1.1	18.8
	2023	1037.2	−20.8	0.1	−24.3	1.1	4.5
	2043	1037.3	−22.9	0.1	−24.4	1.2	4.6
	4320	1047.4	−22.7	0.1	−24.6	0.9	6.2
station S4							
51°52′ S	40	1027	−23.3	1.3	N.D.	N.D.	
00°00′ E	80	1027.3	−24.3	3.1	−26.5	17.7	14.8
	100	1027.4	−24.9	2.3	−26.4	15.7	12.8
	125	1027.6	−25.0	1.1	−26.2	14.2	7.1
	165	1028.1	−25.6	0.4	−26.4	5.6	7.5
	400	1029.5	−26.1	0.1	−26.7	3.5	3.1
	749	1031.2	N.D.	N.D.	−27.2	2.8	
	1108	1033	−24.6	0.1	−26.7	2.9	2.4
	2468	1039.2	−23.5	0.0	−27.2	2.8	1.7
station S5							
57°33′ S	50	1027.6	−29.1	6.6	−28.9	18.9	25.8
00°03′ E	90	1028	−29.7	2.5	−28.6	13.9	15.1
	125	1028.2	−30.3	1.7	−28.9	8.4	16.9
	300	1029.2	−28.0	0.0	−28.7	3.2	1.2
	500	1030.2	−25.4	0.1	−28.2	1.9	4.4
	650	1030.8	−26.4	0.1	−28.5	4.6	3.1
	1500	1034.9	−22.9	0.1	−26.8	0.8	11.4
	2500	1039.4	−24.3	0.0	−27.4	1.5	1.6
	3884	1045.6	−22.8	0.0	−27.9	2.7	1.1
	3894	1045.6	−23.8	0.0	−26.3	0.5	6.4

Selected sterols and their δ^{13}C in the Southern Ocean water column

A.-J. Cavagna et al.

Table 2. Small particles (53 >> 1 µm): δ^{13}C (‰) and concentrations (ng L^{-1}) of cholesterol and brassicasterol. Standard error propagation on δ^{13}C (±1σ) is calculated via FREML regression correction (see e.g. method section). N.D. means no data.

	depth (m)	density (g L^{-1})	δ^{13}C$_{cholesterol}$ (‰)	cholesterol (ng L^{-1})	δ^{13}C$_{brassicasterol}$ (‰)	brassicasterol (ng L^{-1})	bra/cho (no unit)
station S1							
36°31′ S	50	1025.9	−27.6 ± 1.2	37,6	−25.8 ± 1.5	65.3	1.7
13°07E	75	1026.4	−25.0 ± 1.1	24.8	−27.7 ± 1.2	42.1	1.7
	125	1026.9	−26.6 ± 1.1	18,0	−26.7 ± 1.1	17.3	1.0
	250	1027.7	−22.6 ± 1.1	9.8	−25.2 ± 1.1	6.5	0.7
	750	1030.5	−23.7 ± 1.1	7.1	–	–	
	1250	1033.3	−21.5 ± 1.1	3.0	–	–	
	2750	1040.3	−20.9 ± 1.1	2.3	–	–	
	4700	1049.0	-21.4 ± 1.1	2.7	–	–	
station S2							
42°28′ S	30	1026.2	−26.8 ± 1.1	33.8	−27.4 ± 1.1	46.8	1.4
08°55′ S	75	1026.7	−27.0 ± 1.1	24.5	−26.6 ± 1.1	30.1	1.2
	130	1027.2	−29.4 ± 1.2	8.8	−29.0 ± 1.2	9.3	1.1
	250	1028	−28.9 ± 1.2	8.1	−30.1 ± 1.3	6.9	0.9
	590	1029.8	−31.0 ± 1.3	5.1	−30.3 ± 1.3	3.7	0.7
	608	1030.1	−30.3 ± 1.3	6.1	−28.1 ± 1.2	3.4	0.5
	1450	1034.4	−23.7 ± 1.1	1.3	–	–	
	2900	1041	−20.3 ± 1.1	0.7	–	–	
	2910	1041.1	−23.9 ± 1.1	0.8	–	–	
	3940	1045.7	−18.2 ± 1.1	0.7	–	–	
station S3							
47°33′ S	20	1026.6	−37.1 ± 1.6	7.4	−36.9 ± 1.6	38.9	5.3
04°22′ S	50	1026.7	−31.5 ± 1.3	17.3	−34.9 ± 1.5	37.8	2.2
	150	1027.6	−30.0 ± 1.2	5.0	−31.2 ± 1.3	7.8	1.6
	230	1028.2	−30.0 ± 1.2	3.9	−31.2 ± 1.3	5.8	1.5
	450	1029.5	−30.6 ± 1.2	3.3	−30.2 ± 1.3	3.7	1.1
	550	1030	−30.4 ± 1.2	6.0	−30.7 ± 1.3	4.4	0.7
	1060	1032.5	−29.7 ± 1.2	2.9	−31.1 ± 1.3	1.6	0.6
	1088	1032.6	−27.3 ± 1.1	1.8	−30.0 ± 1.3	1.5	0.8
	2023	1037.2	−29.7 ± 1.2	0.9	−29.3 ± 1.2	0.7	0.7
	2043	1037.3	−27.8 ± 1.1	1.0	−29.2 ± 1.2	0.9	1.0
	4320	1047.4	−26.4 ± 1.1	0.3	−30.9 ± 1.3	0.3	1.0
station S4							
51°52′ S	80	1027.3	−34.3 ± 1.4	20.1	−35.8 ± 1.5	32.8	1.6
00°00′ E	100	1027.4	−35.5 ± 1.5	13.0	−37.0 ± 1.6	32.7	2.5
	125	1027.6	−33.8 ± 1.4	15.6	−35.70 ± 1.5	29.6	1.9
	165	1028.1	−32.8 ± 1.3	6.2	−40.0 ± 1.8	9.7	1.6
	400	1029.5	−34.3 ± 1.4	2.9	−37.5 ± 1.6	3.4	1.2
	749	1031.2	−32.7 ± 1.3	5.9	−36.3 ± 1.6	2.2	0.4
	1108	1033	−32.8 ± 1.3	1.1	−32.8 ± 1.4	1.3	1.2
	2468	1039.2	−30.1 ± 1.2	1.0	−33.9 ± 1.4	1.1	1.2
station S5							
57°33′ S	50	1027.6	−37.0 ± 1.6	15.8	−40.6 ± 1.8	28.7	1.8
00°03′ E	90	1028	−36.8 ± 1.6	16.0	−40.9 ± 1.8	25.6	1.6
	125	1028.2	−36.8 ± 1.6	9.8	−39.8 ± 1.8	14.7	1.5
	300	1029.2	−34.2 ± 1.4	6.1	−37.1 ± 1.6	10.5	1.7
	500	1030.2	−32.9 ± 1.3	5.6	−37.3 ± 1.6	4.6	0.8
	650	1030.8	−33.5 ± 1.4	3.2	−37.7 ± 1.6	3.3	1.0
	1500	1034.9	N.D.	N.D.	−35.1 ± 1.5	0.8	
	2500	1039.4	−30.7 ± 1.2	0.8	−34.9 ± 1.5	0.7	0.9
	3884	1045.6	−30.4 ± 1.2	0.6	−33.5 ± 1.4	0.6	1.1
	3894	1045.6	−31.2 ± 1.2	0.5	−35.6 ± 1.5	0.7	1.2

Table 3. Large particles (>53 µm): δ^{13}C (‰) and concentrations (ng l^{-1}) of cholesterol and brassicasterol in the upper part of the water column. Standard error propagation on δ^{13}C ($\pm1\sigma$) is calculated via FREML regression correction (see e.g. method section). No results are available for station S3 since the amount of material collected was too small to permit analysis.

	depth (m)	(‰) $\delta^{13}C_{cholesterol}$	(ng l^{-1}) cholesterol	(‰) $\delta^{13}C_{brassicasterol}$	(ng l^{-1}) brassicasterol	bra/cho (no unit)
station S1						
36°31′ S	50	−27.2 ± 1.1	1.14	−28.0 ± 1.2	1.17	1.0
13°07E	75	−27.2 ± 1.1	1.13	–	–	
	125	−29.1 ± 1.2	1.21	−31.4 ± 1.3	1.31	1.1
station S2						
42°28′ S	30	−30.2 ± 1.3	1.25	−29.9 ± 1.2	1.22	1.0
08°55′ S	75	−29.1 ± 1.2	1.21	−29.0 ± 1.2	1.20	1.0
	608	−31.8 ± 1.3	1.33	–	–	
station S4						
51°52′ S	40	−37.1 ± 1.6	1.60	−49.0 ± 1.3	1.31	0.8
00°00′ E	80	−36.1 ± 1.5	1.53	−45.3 ± 2.1	2.06	1.3
	100	−38.5 ± 1.7	1.69	−46.7 ± 2.2	2.15	1.3
	125	−33.8 ± 1.4	1.40	−37.3 ± 1.6	1.61	1.2
station S5						
57°33′ S	50	−37.0 ± 1.6	1.59	−41.9 ± 1.9	1.87	1.2
00°03′ E	90	−42.4 ± 2.0	1.95	−44.8 ± 2.0	2.03	1.0

Table 4. Mixed layer depth MLD (m), sea surface temperature, surface CO_2 aq. concentration (µmol kg^{-1}), surface δ^{13}C (‰) for LP and SP-POC, LP and SP-cholesterol, LP and SP-brassicasterol. Standard deviation ($\pm 1\sigma$) is the average standard deviation with one exception (*) = analytical standard error ($\pm 1\sigma$). STZ = Sub-Tropical Zone, SAZ = Sub-Antarctic Zone, PFZ = Polar Frontal Zone, IPFZ = Intermediate Polar Frontal Zone (also named Southern Antarctic Circumpolar Current Front SACCF), and WG = Weddell Gyre.

station	latitude	longitude	SO region	mixed layer depth (m)	surface water SST (°C)	(I) surface water [CO2]aq. (µmol kg^{-1})	δ^{13}C cholesterol large particles	δ^{13}C cholesterol small particles	δ^{13}C brassicasterol large particles	δ^{13}C brassicasterol small particles	δ^{13}C POC large particles	δ^{13}C POC small particles
S1	36°31′ S	13°07′ E	STZ	40	20.2 ± 0.7	10.7 ± 0.3	−27.2 ± 0.0	−27.1 ± 0.7	−28.0 ± 1.2	−26.7 ± 1.3	−21.2 ± 0.7	−20.9 ± 0.1 (*)
S2	42°28′ S	08°55′ E	SAZ	50	13.2 ± 0.3	13.7 ± 0.5	−29.7 ± 0.7	−26.9 ± 0.1	−29.5 ± 0.6	−27.0 ± 0.6	−20.1 ± 0.6	−21.9 ± 0.6
S3	47°33′ S	04°22′ E	PFZ	100	6.4 ± 0.1	18.1 ± 0.2	no data	−34.3 ± 4.0	no data	−35.9 ± 1.4	−25.3 ± 0.2	−25.0 ± 0.1
S4	51°52′ S	00°00′ E	IPFZ	100	2.4 ± 0.3	20.7 ± 0.2	−37.2 ± 1.2	−34.9 ± 0.8	−47.0 ± 1.9	−36.4 ± 0.8	−24.2 ± 0.8	−26.4 ± 0.1
S5	57°33′ S	00°03′ E	WG	80	0.39 ± 0.01	24.0 ± 0.3	−39.7 ± 3.8	−36.9 ± 0.1	−43.3 ± 2.0	−40.7 ± 0.2	−29.4 ± 0.5	−28.7 ± 0.2

(I) data from Gonzáles–Dávila et al. (2011)

Table 5. Slope, standard error, p-value and R^2 for variation of δ^{13}C (‰), POC large particles, small particles, cholesterol and brassicasterol in small particles vs. surface CO_2 aq. content, for the arbitrary defined surface water (0–100 m), mesopelagic layer (100–1000 m) and deep ocean (1000 -seafloor).

	slope	p-value	R^2
δ^{13}C-POC large particles			
surface water	-0.62 ± 0.12	<0.05	0.81
mesopelagic layer	-0.48 ± 0.04	<0.05	0.97
deep ocean	-0.25 ± 0.04	<0.05	0.88
δ^{13}C-POC small particles			
surface water	-0.60 ± 0.04	<0.05	0.99
mesopelagic layer	-0.47 ± 0.05	<0.05	0.90
deep ocean	-0.48 ± 0.08	= 0.05	0.92
δ^{13}C-cholesterol small particles			
surface water	-0.84 ± 0.13	<0.05	0.91
mesopelagic layer	-0.73 ± 0.10	<0.05	0.86
deep ocean	-0.88 ± 0.14	<0.05	0.89
δ^{13}C-brassicasterol small particles			
surface water	-1.13 ± 0.14	<0.05	0.94
mesopelagic layer	-0.94 ± 0.20	>0.05	0.83
deep ocean	-0.79 ± 0.17	>0.05	0.90
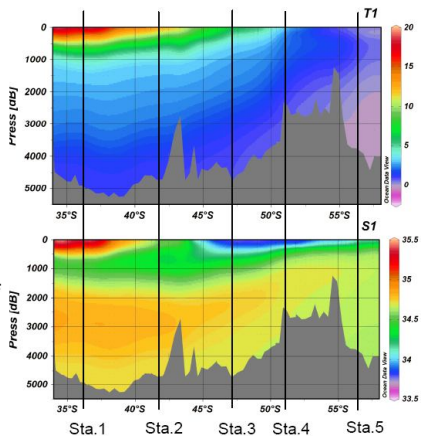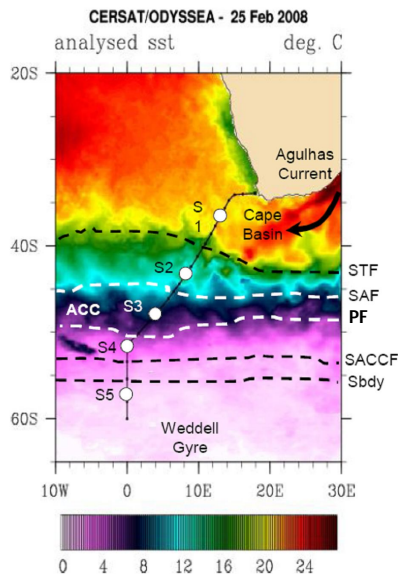
Fig. 1. Left part of panel = BONUS-GoodHope voyage track and super station locations (S1 at 36°31′ S; S2 at 42°28′ S; S3 at 47°33′ S; S4 at 51°52′ S; S5 at 57°33′ S). The background is Sea Surface Temperature SST (°C) from the CERSAT/ODYSSEA satellite. A SST scale is given at the bottom of the image. The north-south gradient in SST is typical of the region in summer. Approximate location of ACC fronts in summer (STF = Sub-Tropical Front, SAF = Sub-Antarctic Front North, PF = Polar Front, SACCF = South Antarctic Circumpolar Current Front, Sbdy = southern boundary of the ACC) are shown. The area north of the STF is the Sub-Tropical Zone (STZ); the Sub-Antarctic Zone (SAZ) is located between STF and SAF; the Polar Front Zone (PFZ) is located between the SAF and PF; the Antarctic Zone (AZ) is located between the PF and Sbdy, and south of the Sbdy is identified as the northern part of the Weddell Gyre (WG). Right part of panel = Complete salinity S1 PSU (lower panel) and temperature T1 (°C, upper panel) sections during BGH (from BGH cruise report; courtesy from *S. Speich*). Station locations are shown.

Title Page

Abstract | Introduction

Conclusions | References

Tables | Figures

|◄ | ►|

◄ | ►

Back | Close

Full Screen / Esc

Printer-friendly Version

Interactive Discussion
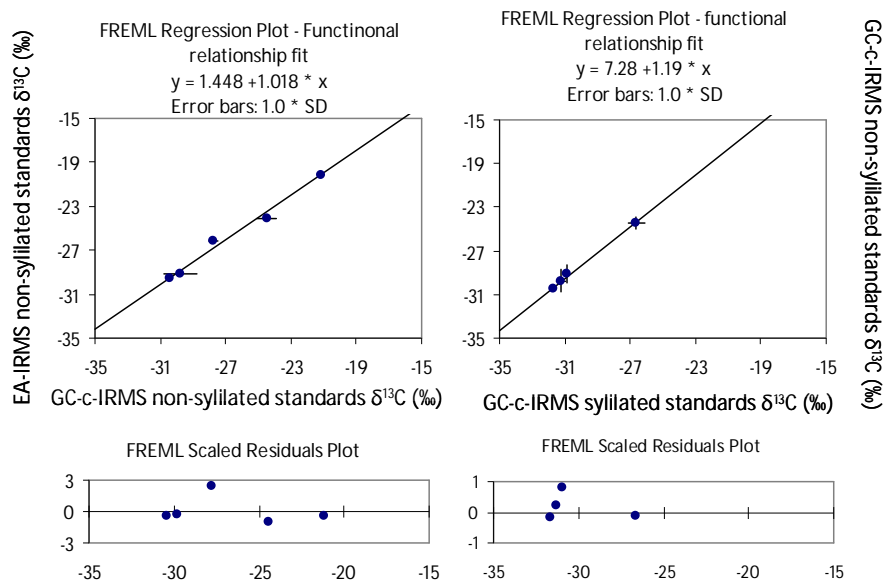
Fig. 2. Standard mix based functional relationship fit for accuracy **(A)** syliation vs. non-sylilation, **(B)** GC-c-IRMS vs. EA-IRMS, and their respective FREML scaled residuals plot.
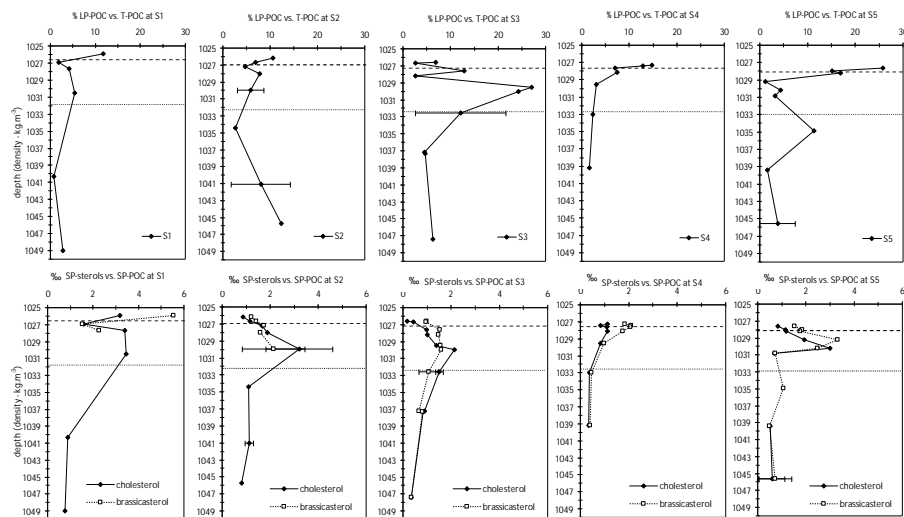
Fig. 3. Upper panel: profiles of large particle (>53 μm) POC content over total POC content (in %). Lower panel: profiles of small particle (1<<53 μm) cholesterol and brassicasterol content over small particle POC content (in ‰). Y-axis depth is shown as seawater density; the 100 m (dashed line) and 1000 m (dotted line) depth horizons are shown. The standard error is estimated as ±30 % for brassicasterol and cholesterol. Error bars shown represent the average standard deviation (±1σ_{SD}) for two close by samples (see also Tables 1 and 2).
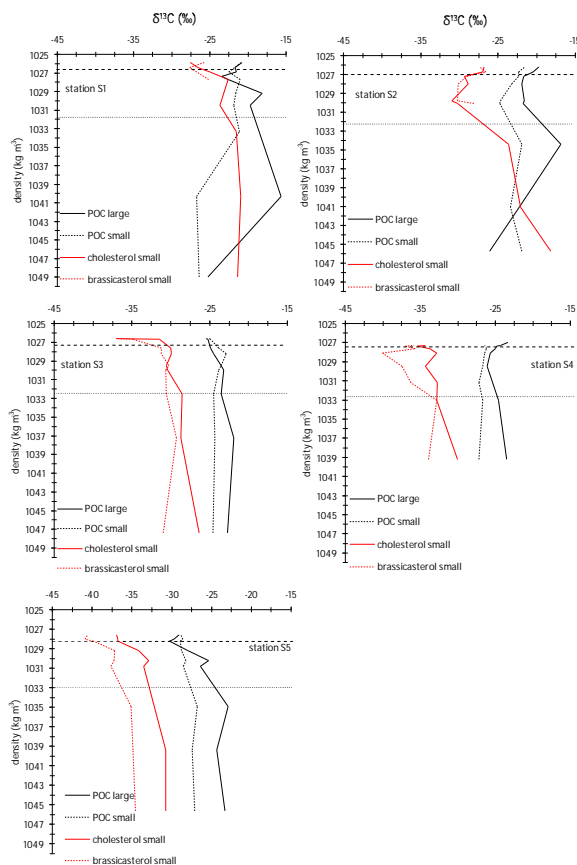
Fig. 4. Profiles of $\delta^{13}C_{POC}$ (‰) for large (>53 µm) and small (1<<53 µm) particles, $\delta^{13}C_{cholesterol}$(‰) and $\delta^{13}C_{brassicasterol}$ (‰) for small particles vs. seawater density. Each panel represents depth profiles per station. Horizontal lines = the 100 and 1000 m horizons.
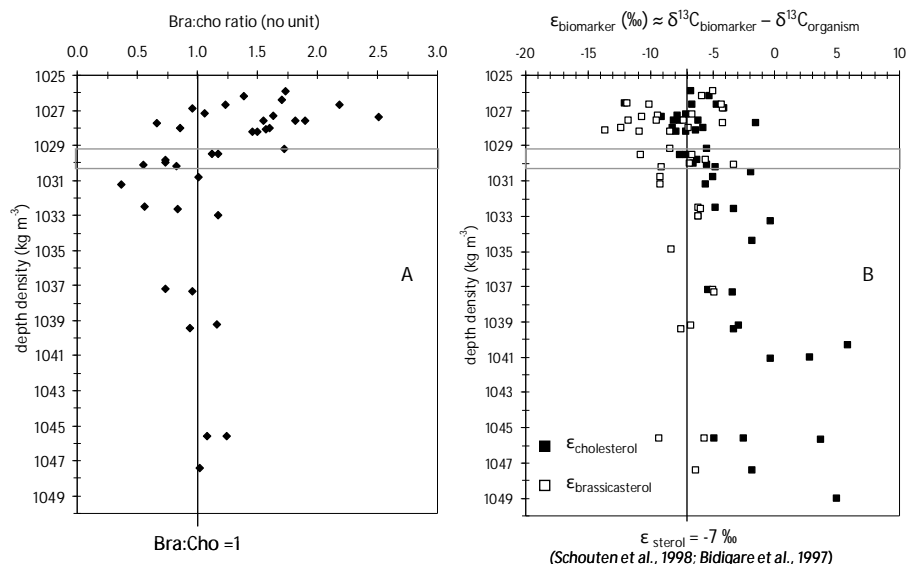
Fig. 5. Panel A = vertical profile of small particle brassicasterol vs. cholesterol concentrations ratio (no unit; from Table 2) for the whole dataset. Panel B = vertical profile of $\varepsilon_{\text{cholesterol}}$ and $\varepsilon_{\text{brassicasterol}}$ for the whole dataset ($\varepsilon_{\text{sterol}}$ (‰) = $\delta^{13}C_{\text{sterol}} - \delta^{13}C_{\text{SP–POC}}$). The grey rectangle represents the range of 500 m depth horizons along the transect (see Table 2).
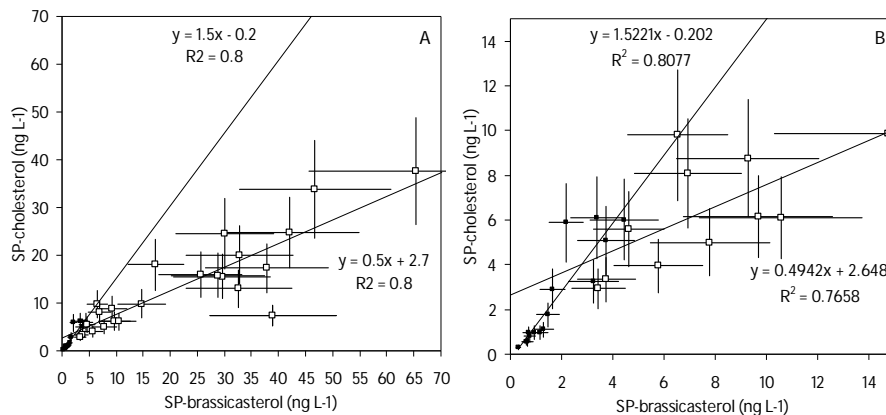
Fig. 6. Correlation between SP-cholesterol and SP-brassicasterol concentrations (panel B is a zoom of panel A) for the whole dataset. Data are spread in two groups: upper 500 m (white squares) and lower 500 m (black squares) following observation of Fig. 5 (see Discussion part 4.1.)
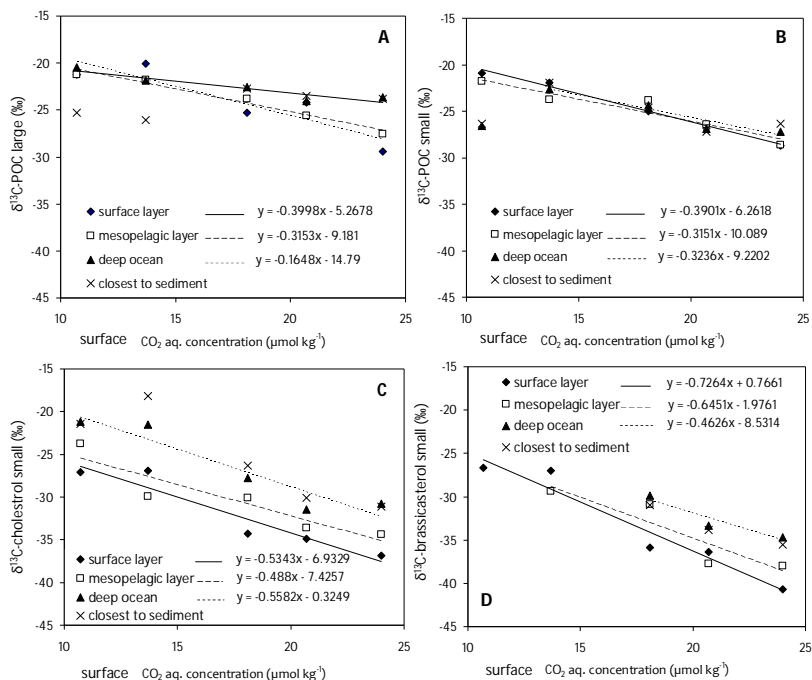
Fig. 7. Upper panel: relationship between surface water (0–100 m) CO2 $_{aq.}$ concentration (µmol kg^{-1}, Table 4) and $\delta^{13}C_{POC}$ (‰) in large (>53 µm) **(A)** and small (1 << 53 µm) **(B)** particles in surface water (0–100 m, closed diamonds), mesopelagic layer (100–1000 m, open square), deep ocean (>1000 m, closed triangles), and bottom waters (crosses). Lower panel: relationship between surface water CO2 $_{aq.}$ concentration and small particles (1 << 53 µm) $\delta^{13}C_{cholesterol}$ **(C)** and $\delta^{13}C_{brassicasterol}$ **(D)** in surface water (0–100 m, closed diamonds), mesopelagic layer (100–1000 m, open square), deep ocean (>1000 m, closed triangles), and bottom water (crosses). Averages (±1σ) are given in Table 5. Standard errors are not shown here for sake of clarity.

Title Page

Abstract | Introduction

Conclusions | References

Tables | Figures

|◄ | ►|

◄ | ►

Back | Close

Full Screen / Esc

Printer-friendly Version

Interactive Discussion